DOI: 10.1002/ejoc.200800506

The Mechanism of the Stetter Reaction – A DFT Study

Kirsty J. Hawkes[a] and Brian F. Yates*[a]

Keywords: Asymmetric catalysis / Umpolung / Carbenes / Reaction mechanisms / Density functional calculations

On the basis of Breslow's mechanism for benzoin condensation, a model asymmetric Stetter reaction has been investigated using DFT methods. In contrast to the concerted benzoin condensation, after formation of the Breslow intermediate the Stetter reaction is found to be a two-step process in which the rate-determining C–C coupling of the Breslow intermediate and the Michael acceptor precedes final proton transfer. In addition, the enolamine is found to play a significant role in the stereochemistry of the product, with the energy difference between stereoisomers of this intermediate reflected throughout the remainder of the reaction sequence. Consequently, electronic and steric control of the stereochemistry of this intermediate should directly enhance the *ee* values of the product.

Introduction

The formation of carbon–carbon bonds through reverse polarity, or umpolung, catalysis has provided an efficient, non-traditional route to many organic compounds. Recent developments in the field have extended reactions from the well known aldehyde coupling of the benzoin condensation, to coupling of ketones, alkenes, and silyls.[1–4]

While the original reactions were highly versatile, one of the greatest achievements for umpolung catalysis has been the introduction of enantioselectivity.[5] Originally, N-heterocyclic carbenes were employed to unselectively catalyse this class of reactions as early as 1943,[6] however, the isolation of the first free carbene by Arduengo in 1991[7] opened the door to a flurry of research on the synthesis of a wide range of chemically "different" carbenes. The newly found ability to control the electronic and steric properties of N-heterocyclic carbenes flowed through to umpolung catalysis with specifically designed chiral N-heterocyclic carbenes producing highly stereoselective reactions with *ee* values well in excess of 90%.[1,2] As syntheses in pharmaceutical and natural product chemistry require highly stereoselective reactions, these results reflected an exciting advancement.

One particular class of umpolung reactions to enjoy such success has been the C–C coupling between aldehydes and an appropriate Michael acceptor in the Stetter reaction. Originally conceived by Stetter in the 1970's,[8] the first reports of a stereoselective reaction were reported by Enders in 1997 with chiral thiazolylidene based catalysts.[9] Initial yields and stereoselectivity were low, however improvements were quickly made by utilising intramolecular reactions.[10] Recently, Rovis and co-workers have made significant advancements in both the scope and selectivity of the reaction using triazole-based N-heterocyclic carbenes. With yields and *ee* values regularly in excess of 90%, these catalysts have proved to be highly efficient under mild conditions and with high tolerance to substrate changes.[11]

To the best of our knowledge there has been no in-depth theoretical study of the mechanism or the stereochemical selectivity of the Stetter reaction. However there has been extensive experimental and computational research into the mechanism of the umpolung related benzoin condensation. In 1903, Lapworth identified a mechanism for the cyanide catalysed benzoin condensation.[12] In 1958, Breslow recognised the same mechanism could be applicable when thiazolium salts were used as alternative catalysts.[13] Supported by experimental evidence, he proposed the presence of the thiazolylidene carbene, which could react with an aldehyde in the same manner as the cyanide anion (Figure 1).

Several experimental and theoretical investigations have been completed on the Lapworth and Breslow inspired mechanism. Ubiquitous to experimental investigations has been the identification of intermediates early in the catalytic cycle; Lapworth isolated mandelonitrile, the cyanide catalysed equivalent of **2(B)**,[12] while **1(B)** and **2(B)** have been identified by NMR[14,15] and mass spectrometry[16] in thiazolium-catalysed reaction mixtures. Computational studies[17–19] have confirmed the applicability of the mechanism to the extent that Dudding and Houk were able to predict the stereochemistry of asymmetric reactions, albeit with slightly overestimated *ee* values.[18]

Recently, López Calahorra proposed two slightly modified mechanisms in which carbene dimers are the active catalysts in preference to the free carbene.[15,17,20] Experimental evidence for catalysis in the more widely used catalytic

[a] School of Chemistry, University of Tasmania,
Private Bag 75, Hobart TAS 7001, Australia
Fax: +61-3-62262858
E-mail: Brian.Yates@utas.edu.au
Supporting information for this article is available on the WWW under http://www.eurjoc.org or from the author.

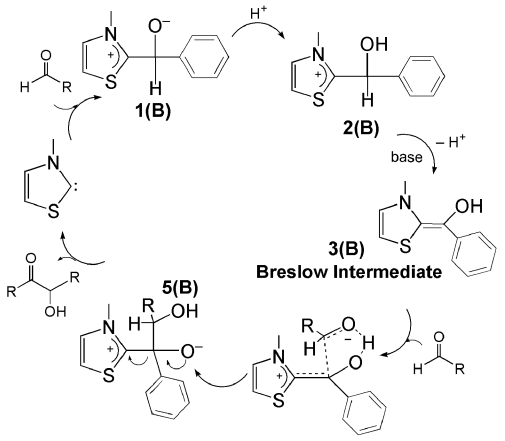

Figure 1. The mechanism for benzoin condensation as first proposed by Breslow [(B) refers to benzoin condensation – see Figure 4 for full numbering scheme].

environments suggested dimers were not necessary for catalysis,[14,16] and indeed, computational results similarly indicated the Breslow mechanism would be more energetically favoured.[18] Despite these results, in conditions favourable for carbene dimer formation a dimer mechanism has not been ruled out.

With the Stetter reaction simply replacing the second aldehyde of the benzoin condensation with a similar conjugate acceptor, it might be expected that the mechanisms for the related reactions are very similar. Overall, on the basis of the Breslow mechanism the reaction can be broken into two sections. The initial phase is identical to the benzoin condensation and involves formation of the "Breslow intermediate", an enolamine formed through the coupling of the aldehyde and carbene catalyst [Figure 2: **0(S)** → **3(S)**]. The second phase of the reaction determines the stereochemistry of the product through C–C coupling of the enolamine and the Michael acceptor [Figure 2: **3(S)** → **0(S)**].

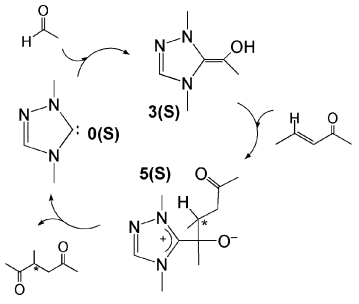

Figure 2. Proposed mechanism for the asymmetric Stetter reaction [(S) refers to Stetter reaction – see Figure 4 for full numbering scheme].

With such excellent stereoselectivity displayed in such a versatile reaction in experiment, a thorough understanding and the ability to predict and manipulate the stereoselectivity of the Stetter reaction would further enhance its application. Accordingly, we present a theoretical study of catalysis for a model Stetter reaction based on the established mechanism for the related benzoin reaction.

Results and Discussion

To get an idea of the important factors affecting the rate and stereochemistry of the asymmetric Stetter reaction in a time-efficient manner, we have used small, prochiral model reactants: 1,3-dimethyltriazolylidene for the carbene catalyst, acetaldehyde for the aldehyde and 3-penten-2-one as the Michael acceptor. These boundaries give a manageable set of reactions in which to gain insight into the underlying reaction mechanism and will be extended to the true stereoselective reactions in future work. Herein, we detail results of the Stetter reaction under these model conditions with an additional focus on the important Breslow intermediate.

Creation of the Enolamine (Steps 0–3)

Experimental results have indicated that the intermediates up to the Breslow intermediate **3** are present in most umpolung catalysis, however there has been little research on the mechanism for the proton transfer between species early in the cycle to create the enolamine. While rearrangement of **1** to form the Breslow intermediate **3** in protic conditions would be straight forward due to the relative ease of "proton hopping", the success of the reaction in aprotic conditions implies another low-energy proton transfer is available to the system in this situation.

Previous computational studies of the mechanism under aprotic conditions have generally assumed a 1,2-hydrogen shift,[17,19,20] however this is a symmetry forbidden and consequently high energy process. Indeed, calculations for our system indicate a barrier of 163.8 kJ mol^{-1}. Further, this 1,2-shift is found to be the lowest energy intramolecular hydrogen transfer available and consequently formation of the Breslow intermediate from **1** is almost certainly an intermolecular process.

Examination of reaction intermediates identified several potential intermolecular proton transfer agents, in particular several zwitterion intermediates and the reacting carbene and aldehyde. Several of these transfers proved to be relatively low energy,[21] however the most favourable interaction is that between two carbene/aldehyde coupled intermediates **1** (Figure 3) reacting with an overall barrier of 55 kJ mol^{-1}. With the rearranged Breslow intermediate **3**, 23 kJ mol^{-1} lower in energy than the reactant **1** and a relatively high catalyst loading, creation of **3** would be expected to be facile, even in aprotic conditions.

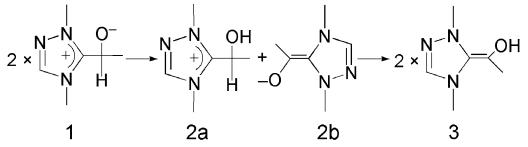

Figure 3. Most favourable intermolecular proton transfer to create the Breslow intermediate (see Figure 4 for full numbering scheme).

The Overall Reaction Profile

In each reaction, there are three entities that affect the stereochemistry of the product: the reacting carbene, the

resulting Breslow intermediate and the reacting Michael acceptor. While the combinations of these different stereochemical possibilities create a vast number of possible interactions, for our initial studies we were able to reduce the complexity with the observation that catalytic runs have found the *Z* form of the reacting Michael acceptor to be far less reactive than the corresponding *E* form. Therefore, we have only used the *E* form in our calculations.

With this in mind, it is the initial interaction of the enolamine intermediate and enone that influence the stereochemistry of the product. The enolamine **3** may have one of two conformations, *E* or *Z*, to which the *si* or *re* side may react with the *si* or *re* side of the Michael acceptor. These interactions result in eight distinct possibilities for C–C coupling, four leading to an *R* product and four to an *S* product (Table 1).

Table 1. Reactant and product stereochemistry.

Reaction label	Enolamine	Enolamine reacting face	Michael acceptor reacting face	Product
ZA	*Z*	*si*	*re*	*R*
ZB	*Z*	*si*	*si*	*S*
ZC	*Z*	*re*	*si*	*S*
ZD	*Z*	*re*	*re*	*R*
EA	*E*	*re*	*si*	*S*
EB	*E*	*re*	*re*	*R*
EC	*E*	*si*	*re*	*R*
ED	*E*	*si*	*si*	*S*

After an exhaustive study of the potential-energy surface, our calculations show that the full route for Stetter catalysis in an aprotic solvent and with a preformed carbene catalyst can be described by Figure 4, with the lowest overall energy coming from the *E* form of the enolamine.

Several important observations can be made from these results. Firstly, with identical methyl groups as nitrogen substituents on the enolamine, orbital overlap between the *si* face of the *Z* enolamine and *si* face of the enone (Figure 5: Model ZB) is a mirror image of the reaction for the *re* face of the *Z* enolamine and *re* face of the enone (Figure 5: Model ZD). Consequently, these reactions are energetically equivalent despite resulting in products with opposite stereochemistry. Similarly, the pairs ZA/ZC, EA/EC, and EB/ED are energetically degenerate and the eight possible interactions between the *si* and *re* faces of the enolamine and enone in Table 1 collapse into four energy categories for the reaction (Figure 6: **3** → products).

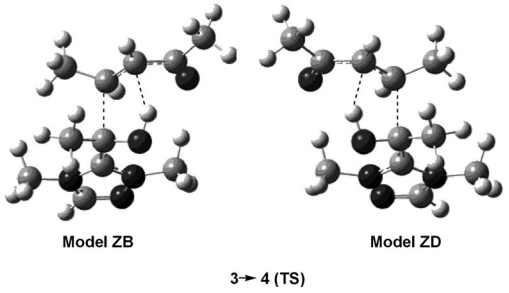

Figure 5. Mirror image transition structures for reactions ZB and ZD.

Secondly, regardless of the stereochemistry of the reactants and intermediates, the overall reaction displays a con-

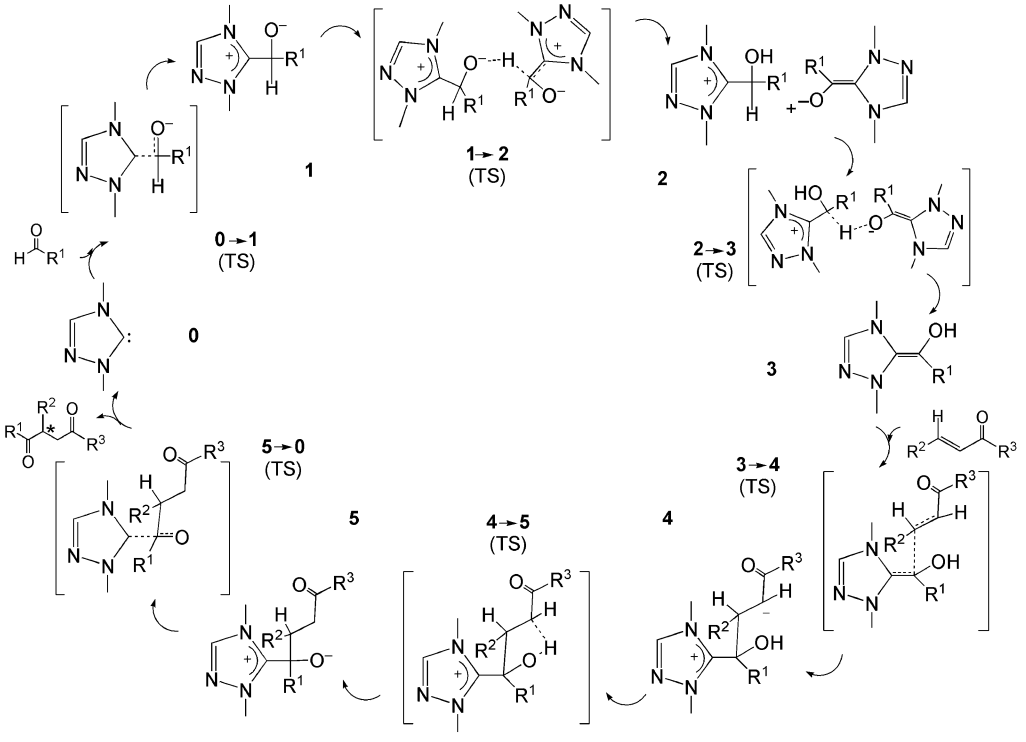

Figure 4. Overall mechanism for the Stetter reaction.

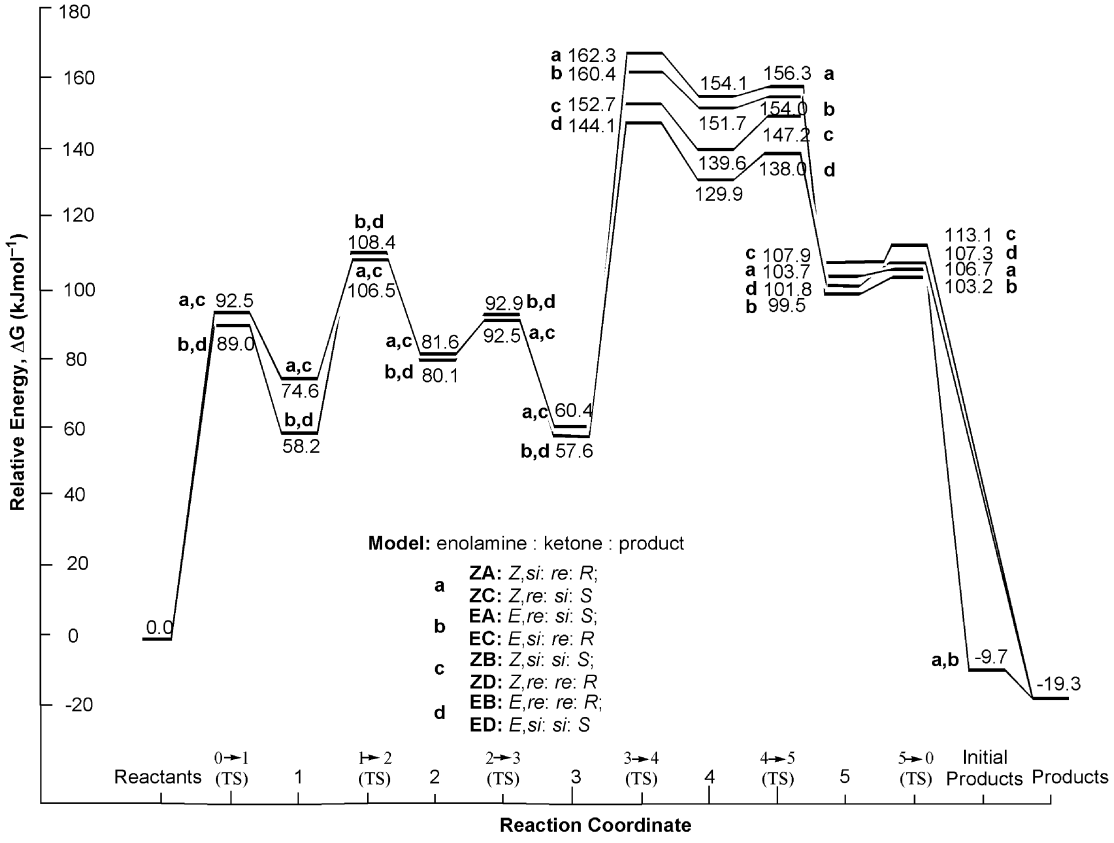

Figure 6. Energies for stereochemical coupling.

sistent reaction path with the overall rate-determining step being the stereochemical determining C–C coupling step itself (Figure 6, **3** → **4 TS**). This result is particularly interesting as our model assumes aprotic conditions, and the creation of the enolamine **3** is expected to be even less demanding with a freely available proton source.

Thirdly, while calculations on the benzoin condensation showed a concerted one-step C–C coupling and hydrogen transfer between the Breslow intermediate and second aldehyde[18] [Figure 1: **3(B)** → **5(B)**], the Stetter reaction appears to be a two-step process in which C–C coupling (**3** → **4**) precedes hydrogen transfer (**4** → **5**). In each case, the C–C coupled intermediate **4** is stabilised by hydrogen bonding of the OH group to the newly created carbanion and proton transfer is therefore unhindered and driven by a more thermodynamically stable product.

The final important observation is the energy differences between the different reaction pathways for **3** to **5**. Each isomer of the Breslow intermediate leads to a higher (**a**: ZA/ZC and **b**: EA/EC) and lower (**c**: ZB/ZD and **d**: EB/ED) energy reaction path (Figure 6). The LUMO of the Michael acceptor is identical for the *si* and *re* faces and hence good overlap can occur between the HOMO of the enolamine and either side of the Michael acceptor. Consequently, the lowest energy pathway for a particular isomer of the enolamine is that in which the steric interactions of the enolamine *N*-substituents and the Michael acceptor are at a minimum (Figure 7).

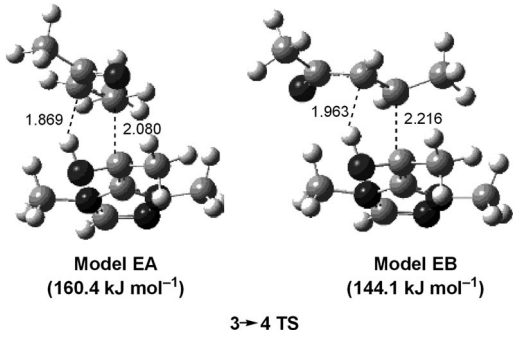

Figure 7. Example higher (EA) and lower (EB) energy C–C coupling transition structures (bond lengths in Å).

In addition, the *Z* isomer pathways are consistently higher in energy than their *E* isomer counterparts (**a** > **b** and **c** > **d** in Figure 6), and generally the differences are consistent with the energy difference between the *Z* and *E* forms of the enolamine intermediate **3**. Conceivably, with little separation between the energies of these isomers, two pathways to C–C coupling that lead to opposite stereochemistry in the product will be very close in energy and therefore lead to a non-selective overall process. Alternatively, by increasing the energy difference between the *E* and *Z* forms of the enolamine it may be possible to increase the gap between these competing pathways, consequently favouring one particular pathway and increasing the overall stereoselectivity.

Therefore, we now focus on the factors influencing the *E* to *Z* ratio of the enolamine.

Stereochemistry of the Enolamine 3

The above results indicate the biggest factor affecting overall stereoselectivity may be the energy difference between the *E* and *Z* isomers of the Breslow intermediate. Previous theoretical results for the benzoin condensation have indicated the *E* form of the enolamine is more stable than the *Z* form although no explanation was offered. With both isomers displaying a preference for the OH group directed away from the triazole ring in our system (Figure 8),[22] there remains a 3 kJ mol^{-1} energy difference between the *E* and *Z* isomers.

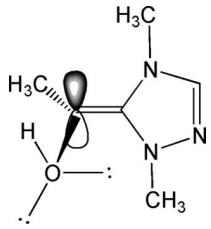

Figure 8. Optimised rotation of the enolamine OH bond.

Several low-energy resonance forms are available to help stabilise each isomer of the enolamine (Figure 9). A rudimentary indication of the relative stability of each of these resonance forms can be achieved by enforcing "pure" bond lengths, where each bond is set to average experimental distances for a specific bond order, and optimising each resulting structure. In so doing, it is clear that the neutral resonance form **3** is the most stable and would be dominant in the equilibrium geometry (Table 2). The relative stability of the possible zwitterions is as expected, with the negative charge most readily accommodated directly on the electronegative nitrogen (resonance form **2**). The two carbanion forms **1** and **5** are very similar, with **5** slightly less favoured due to the proximity of the cation to the electronegative nitrogen N^4. Resonance form **4** is highly unfavoured with an unstable carbanion located on the backbone of the azole ring. Overall, it is expected that the equilibrium geometry would reflect these stabilities (vide infra), with a strong contribution from resonance form **3** and minor contributions observed for the remaining zwitterions.

Table 2. Energies of enolamine resonance forms relative to the optimised *E* structure.

	Relative energy [kJ mol^{-1}]	
Structure	*E*	*Z*
Optimised geometry	**0**	**3**
Resonance **1**	98	105
Resonance **2**	90	100
Resonance **3**	19	23
Resonance **4**	120	117
Resonance **5**	107	104

Within each resonance form, the oxygen lone pairs as depicted in Figure 8 play a small, yet significant, role in whether the *E* or *Z* form is favoured. By providing extra electron density, the oxygen lone pairs have a slightly destabilising effect when located on the same side of the molecule as other areas of high electron density, in particular the nitrogen lone pairs. Conversely, the interaction from the lone pairs is somewhat stabilising when located adjacent to areas of low electron density, such as the nitrogen cations. Consequently, the *E* conformers of resonance structures **1** and **2** are found to be more stable than their corresponding *Z* forms, while the reverse is true for resonance structures **4** and **5** where the *Z* conformation is favoured.

Overall, the combination of cation/anion stability and oxygen lone pair interactions leads to theoretical resonance contributions for our model enolamine in the order:

E3 > Z3 >> E2 > E1 > Z2 > Z5 > Z1 > E5 > Z4 > E4

Examination of bond lengths and angles (Figure 10) combined with an NBO analysis[22] for the optimised geometry of each form of the enolamine confirmed the contributions of each of these resonance structures. Both the *E* and *Z* forms show high contributions from resonance form **3** with only slightly elongated C^5=N^4 and C^2=C double bonds. As expected, only minor contributions are found for the remaining resonance forms with all other bond lengths closer to single bonds. In spite of their less obvious contribution, there remain some important effects from these minor resonance forms. Most significantly, for both *E* and *Z* conformers the strength of contribution from resonance form **2** and, to a lesser degree, resonance form 1 result in an almost planar sp^2 hybridised N^1, while N^3 retains sp^3 hybridisation due to the weaker contribution of resonance forms **4** and **5**.

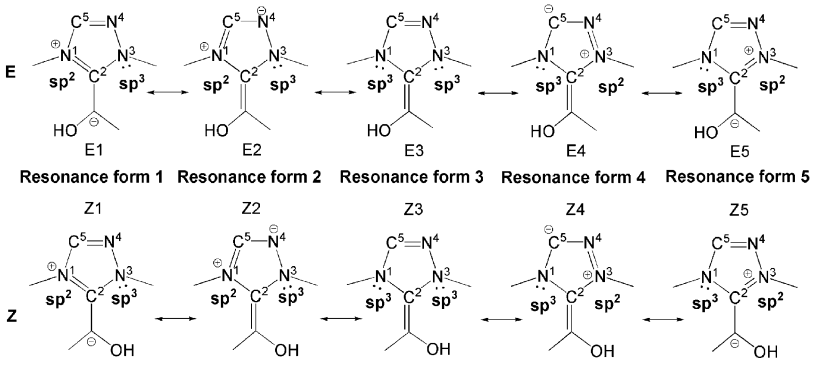

Figure 9. Enolamine resonance forms.

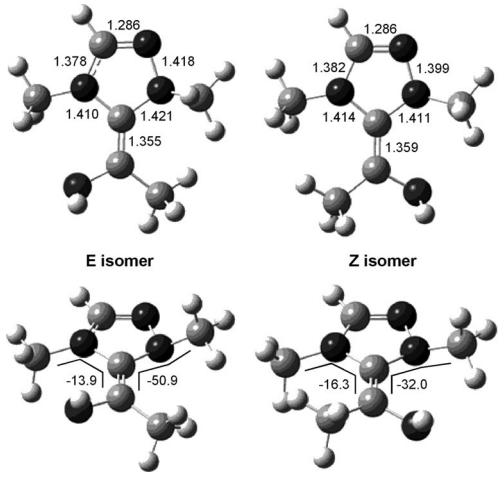

Figure 10. Bond lengths [Å] and angles [°] for the optimised *E* and *Z* enolamines.

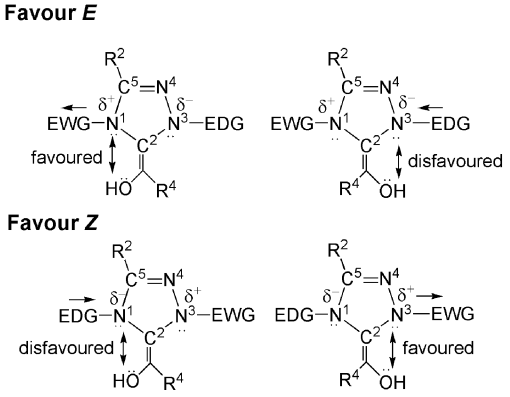

Figure 11. Electronic influence on the *E* and *Z* conformers.

By considering the characteristics of the various resonance forms, the energy difference between the *E* and *Z* forms of the enolamine may be enhanced by modifying the substituents around the carbene ring. While electronic changes will affect the stability of each of the minor resonance forms, the key to separating the *E* and *Z* energy ratios is to increase the effect of the nitrogen/oxygen lone pair interactions, in particular for the main resonance form **3**. To this end, electron withdrawal on the side of the oxygen is expected to decrease the nitrogen/oxygen pair interaction and electron donation to increase it (Figure 11). Indeed, calculations to test this hypothesis show that simple substitution of the N^1 and N^3 substituents can enhance (Table 3: Entry 2) or decrease (Table 3: Entry 3) the stability of the *E* isomer with respect to the *Z*.

While these results indicate success in favouring the *E* form of the enolamine, the *Z* form can only be significantly favoured if the carbanion in the "*Z* preferred" resonance form **4** is stabilised to the same degree as the nitrogen anion of resonance form **2**. Indeed, by including an electron withdrawing group in the C^5 position alone, the energy difference between the *E* and *Z* conformers is a non-distinguishable 0.2 kJ mol^{-1} (Table 3: Entry 4). Combining the anion stabilising C^5 substitution with the favoured N^1 and N^3 electronic changes results in the *Z* conformer being more stable than the *E* by 4.2 kJ mol^{-1} (Table 3: Entry 5).

With a clearer idea of the subtle part that electronic effects play in the enolamine, consideration of the role of the steric interactions on the *E* to *Z* energy ratio becomes important. In the absence of a strong electron withdrawing group on C^5, results indicate that nitrogen N^1 will preferentially adopt sp^2 hybridisation and N^3 sp^3 hybridisation (Figure 10). With this in mind, it becomes clear that any movement of the nitrogen substituents to decrease possible steric interactions will be more easily accommodated on N^3, as N^1 movement potentially disrupts the π system and electronic stability provided by resonance forms **1** and **2**.

Indeed, substitution on N^3 was found to have little effect on the ratio of *E* to *Z* stability with movement of the N^3 substituent to minimise steric interactions having little impact on the overall electronic properties (Table 4). Conversely, substitution of the bulky ^{t}Bu group on the aldehyde (R^4) or N^1 nitrogen (R^1) indicated a strong favouring of the *E* form, where the smaller OH group is located next to the almost planar sp^2 hybridised N^1–R^1, and the sp^3 hybridised N^3–R^3 bending out of the way of the bulk on the aldehyde. The *Z* form however is significantly destabilised as it en-

Table 4. Steric influences on enolamine *E* to *Z* energy ratios.

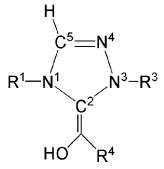

Description	R^1, R^3 and R^4	Energy of *Z* compared to *E* [kJ mol^{-1}][23]
Original model	$R^1 = R^3 = R^4$ = Me	2.8
Bulk on aldehyde	$R^1 = R^3$ = Me; R^4 = tBu	11.7
Bulk on N^1 (sp^2-hybridised)	$R^3 = R^4$ = Me; R^1 = tBu	12.6
Bulk on N^3 (sp^3-hybridised)	$R^1 = R^4$ = Me; R^3 = tBu	2.7

Table 3. Energy changes of *E* to *Z* ratio with substituent alteration.

Entry	N^1 substituent	C^5 substituent	N^3 substituent	Favoured isomer	Energy difference [kJ mol^{-1}]
1	Me	H	Me	*E*	2.8
2	*p*-CN-Ph	H	*p*-OMe-Ph	*E*	6.2
3	*p*-OMe-Ph	H	*p*-CN-Ph	*E*	0.5
4	Me	CN	Me	*E*	0.2
5	*p*-OMe-Ph	CN	*p*-CN-Ph	*Z*	4.2

counters enhanced steric repulsion between R^1 and R^4 and sacrifices some of the sp^2 hybridisation and, hence, the contribution from the more electronically stable resonance forms **1** and **2**.

Implications from the Model Reaction

To date, experimental umpolung catalysts have enhanced stereoselectivity by increasing steric bulk on one face of the enolamine to promote exclusive reaction on the opposing face,[1,3,5,9,11,24] however the exact conformation of the enolamine has not been considered. Combined, the steric and electronic results herein indicate the balance between the *E* and *Z* isomers, which potentially lead to opposite stereochemical products, may not be as straight forward as expected, although tailoring the carbene substituents both electronically and sterically can be used to influence this ratio.

In particular, for the triazole systems changes to favour the *E* form become more straight forward due to the relative stability of the underlying resonance forms. In the most basic sense, this may be achieved through bulky, electron withdrawing substituents on N^1, steric bulk on the aldehyde, or electron donating N^3 substituents. Conversely, the *Z* form is only significantly favoured with strong electron withdrawing groups stabilising the carbanion of resonance structure **4** or **5**, and even then requires the correct combination of electronic properties on the remaining nitrogen substituents to further increase the *Z* to *E* ratio.

While it is acknowledged that experimental catalysts and reactants contain more complicated steric and electronic factors, the relative energies of the *E* and *Z* C–C coupling intermediates and corresponding products is expected to reflect the trends found in our model system and therefore affect the *ee* values found in the true catalytic system.

Similarly, the discovery of the two-step C–C coupling and proton transfer steps has implications for potential side reactions. While correct orientation of the alkene in intermediate **4** indicates a low barrier for proton transfer to form the Stetter product, the two step process suggests competing reactions may become more favourable with a small change in the alkene orientation, potentially decreasing the yield of the Stetter reaction.

We are currently investigating other factors affecting these important intermediates, including solvent effects, side reactions and the true catalysts used in many intramolecular Stetter reactions.[25]

Conclusions

By studying a model reaction involving a simple 1,3-dimethyltriazolylidene carbene catalyst, we have established some important characteristics affecting the Stetter reaction based on the mechanism proposed by Breslow for the benzoin condensation.

The overall mechanism for the Stetter reaction in aprotic conditions appears to be similar to that for the benzoin condensation, however the concerted C–C coupling and hydrogen transfer of the benzoin condensation is split into a two step process in the Stetter reaction. (The impact of this result on alternative pathways and possible side reactions for the Stetter reaction is currently being investigated by our group.)

Even in aprotic conditions, creation of the enolamine Breslow intermediate is relatively straightforward in an intermolecular manner and may occur through a variety of reactant and intermediate interactions in the absence of another suitable proton donor. The calculated rate-determining step of the overall reaction is found to be the stereochemical determining C–C coupling step itself.

With the pathways leading to opposite stereochemical products energetically separated by an amount consistent with the energy difference of the corresponding enolamine isomers, several important characteristics of the enolamine were observed in our study. Firstly, several resonance forms contribute to the stability of the enolamine. While two of these were indeed the "umpoled" zwitterion in which the aldehyde carbon holds a formal negative charge (resonance forms **1** and **5**), these resonance forms contribute only a minor amount to the overall stability of the enolamine, in which the main stability is derived from the true neutral resonance form **3**. Indeed, it is the rearrangement of the HOMO orbital of the aldehyde in a manner conducive to overlap with the LUMO of the Michael acceptor that is responsible for reactivity, as the charge on the activated aldehyde carbon remains similar to that of the free aldehyde.

Similarly, the stability of the *E* and *Z* forms of the enolamine are affected by the resonance forms. Although all five of the main resonance forms are available to both *E* and *Z* conformations, the proximity of the oxygen lone pairs to other areas of high electron density within the carbene ring destabilise the lower energy resonance forms **1** and **2** for the *Z* conformer, while simultaneously stabilising areas of low electron density for the corresponding *E* conformer. Consequently, without altering the relative stability of the individual resonance forms, the *E* form of the enolamine is more stable than the corresponding *Z* form. Similarly, bulky substituents on either the sp^2 hybridised N^1 nitrogen or aldehyde significantly favour the *E* form through separation of steric interactions, with the N^3 substituent less influential on the sp^3 hybridised nitrogen.

These are significant results for future enhancements of umpolung catalysts. By blocking one face of the enolamine and further stabilising the *E* form with respect to the *Z*, it should be possible to control and significantly enhance the stereoselectivity of this important set of reactions.

Computational Details

Initial conformers for all pathways were calculated using GMMX molecular mechanics in the PCModel suite.[26] Full geometry optimisations and harmonic vibrational frequencies for a series of low energy conformers were then calculated at the B3LYP[27] level of theory with the 6-31G(d) basis set on all atoms with the Gaussian 03[28] set of programs. Zero-point vibrational-energy corrections

were obtained using unscaled frequencies. All transition structures contained exactly one imaginary frequency and were characterised by following the corresponding normal mode towards the products and reactants.

Higher level single point calculations were performed on the optimised geometries at the B3LYP level with a 6-311+G(2d,p)[29] basis set. Energies from these single point calculations were combined with the thermodynamic corrections at the lower level of theory to obtain ΔG_{298} numbers. All energies quoted in this paper refer to these final ΔG_{298} values.

Crude resonance structures were obtained by fixing bond lengths using the Gaussian 03 opt = modredundant keyword and by carrying out NBO analysis[30] on optimised structures with constrained bonds and lone pairs using the pop = nboread and $CHOOSE keywords.

Supporting Information (see footnote on the first page of this article): Tables of energies and cartesian coordinates (*XYZ*) for all structures including full details for the creation of the Breslow intermediate (**0** → **3**), enolamine conformers and NBO analysis; complete ref.[28].

Acknowledgments

The authors wish to thank the Australian and Tasmanian Partnerships for Advanced Computing (APAC and TPAC) for super-computing time and the Australian Research Council for funding.

[1] D. Enders, O. Niemeier, A. Henseler, *Chem. Rev.* **2007**, *107*, 5606–5655.
[2] N. Marion, S. Díez-González, S. P. Nolan, *Angew. Chem. Int. Ed.* **2007**, *46*, 2988–3000.
[3] J. Seayad, B. List, *Org. Biomol. Chem.* **2005**, *3*, 719–724.
[4] K. Zeitler, *Angew. Chem. Int. Ed.* **2005**, *44*, 7506–7510.
[5] J. C. Sheehan, D. H. Hunneman, *J. Am. Chem. Soc.* **1966**, *88*, 3666–3667.
[6] T. Ugai, S. Tanaka, S. Dokawa, *J. Pharm. Soc. Jpn.* **1943**, *63*, 296–300.
[7] A. J. Arduengo III, R. L. Harlow, M. Kline, *J. Am. Chem. Soc.* **1991**, *113*, 361–363.
[8] a) H. Stetter, *Angew. Chem. Int. Ed. Engl.* **1976**, *15*, 639–647; b) H. Stetter, M. Schreckenberg, *Angew. Chem. Int. Ed. Engl.* **1973**, *12*, 81.
[9] D. Enders, K. Breuer, J. Runsink, J. H. Teles, *Helv. Chim. Acta* **1996**, *79*, 1899–1902.
[10] E. Ciganek, *Synthesis* **1995**, 1311–1314.
[11] a) M. S. Kerr, J. Read de Alaniz, T. Rovis, *J. Am. Chem. Soc.* **2002**, *124*, 10298–10299; b) M. S. Kerr, T. Rovis, *Synlett* **2003**, 1934–1936; c) J. Read de Alaniz, T. Rovis, *J. Am. Chem. Soc.* **2005**, *127*, 6284–6289; d) N. T. Reynolds, T. Rovis, *Tetrahedron* **2005**, *61*, 6368–6378.
[12] A. Lapworth, *J. Chem. Soc. Trans.* **1903**, *83*, 995–1005.
[13] R. Breslow, *J. Am. Chem. Soc.* **1958**, *80*, 3719–3726.
[14] a) R. Breslow, R. Kim, *Tetrahedron Lett.* **1994**, *35*, 699–702; b) M. J. White, F. J. Leeper, *J. Org. Chem.* **2001**, *66*, 5124–5131.
[15] F. López-Calahorra, R. Rubires, *Tetrahedron* **1995**, *51*, 9713–9728.
[16] W. Schrader, P. P. Handayani, C. Burstein, F. Glorius, *Chem. Commun.* **2007**, 716–718.
[17] J. Martí, F. López-Calahorra, J. M. Bofill, *THEOCHEM* **1995**, *339*, 179–194.
[18] T. Dudding, K. N. Houk, *PNAS* **2004**, *101*, 5770–5775.
[19] B. Goldfuss, M. Schumacher, *J. Mol. Model.* **2006**, *12*, 591–595.
[20] F. López-Calahorra, J. Castells, L. Domingo, J. Martí, J. M. Bofill, *Heterocycles* **1994**, *37*, 1579–1597.
[21] Each reaction is a two-step transfer process; nearly 30 different intermediates and transition structures were studied and full energy pathways are supplied in the Supporting Information
[22] For full details see Supporting Information
[23] Although these numbers are very small, it must be remembered that a change in the difference of the two activation energies from, say, 2.8 to 12.6 kJ mol^{-1} equates to a change in *ee* from 54% to 99%.
[24] a) M. Christmann, *Angew. Chem. Int. Ed.* **2005**, *44*, 2632–2634; b) J. R. de Alaniz, T. Rovis, *J. Am. Chem. Soc.* **2005**, *127*, 6284–6289; c) D. Enders, T. Balensiefer, *Acc. Chem. Res.* **2004**, *37*, 534–541; d) D. Enders, U. Kallfass, *Angew. Chem. Int. Ed.* **2002**, *41*, 1743–1745; e) D. Enders, O. Niemeier, T. Balensiefer, *Angew. Chem. Int. Ed.* **2006**, *45*, 1463–1467; f) M. S. Kerr, T. Rovis, *J. Am. Chem. Soc.* **2004**, *126*, 8876–8877; g) R. L. Knight, F. J. Leeper, *J. Chem. Soc. Perkin Trans. 1* **1998**, 1891–1893; h) X. Linghu, J. R. Potnick, J. S. Johnson, *J. Am. Chem. Soc.* **2004**, *126*, 3070–3071; i) S. M. Mennen, J. D. Gipson, Y. R. Kim, S. J. Miller, *J. Am. Chem. Soc.* **2005**, *127*, 1654–1655.
[25] Initial calculations with a solvent suggest that there are only small changes in the relative energies of **a**, **b**, **c** and **d** in Figure 6.
[26] *PC Model for Windows*, 8.50.0, Serena Software, Bloomington, IN (USA), **2003**.
[27] a) A. D. Becke, *J. Chem. Phys.* **1993**, *98*, 5648–5652; b) R. H. Hertwig, W. Koch, *Chem. Phys. Lett.* **1997**, *268*, 345–351; c) P. J. Stephens, J. F. Devlin, C. F. Chabalowski, M. J. Frisch, *J. Phys. Chem.* **1994**, *98*, 11623–11627.
[28] M. J. Frisch, G. W. Trucks, H. B. Schlegel, G. E. Scuseria, M. A. Robb, J. R. Cheeseman, J. A. Montgomery Jr., T. Vreven, K. N. Kudin, J. C. Burant, J. M. Millam, S. S. Iyengar, J. Tomasi, V. Barone, B. Mennucci, M. Cossi, G. Scalmani, N. Rega, G. A. Petersson, H. Nakatsuji, M. Hada, M. Ehara, K. Toyota, R. Fukuda, J. Hasegawa, M. Ishida, T. Nakajima, Y. Honda, O. Kitao, H. Nakai, M. Klene, X. Li, J. E. Knox, H. P. Hratchian, J. B. Cross, C. Adamo, J. Jaramillo, R. Gomperts, R. E. Stratmann, O. Yazyev, A. J. Austin, R. Cammi, C. Pomelli, J. W. Ochterski, P. Y. Ayala, K. Morokuma, G. A. Voth, P. Salvador, J. J. Dannenberg, V. G. Zakrzewski, S. Dapprich, A. D. Daniels, M. C. Strain, O. Farkas, D. K. Malick, A. D. Rabuck, K. Raghavachari, J. B. Foresman, J. V. Ortiz, Q. Cui, A. G. Baboul, S. Clifford, J. Cioslowski, B. B. Stefanov, G. Liu, A. Liashenko, P. Piskorz, I. Komaromi, R. L. Martin, D. J. Fox, T. Keith, M. A. Al-Laham, C. Y. Peng, A. Nanayakkara, M. Challacombe, P. M. W. Gill, B. Johnson, W. Chen, M. W. Wong, C. Gonzalez, J. A. Pople, *Gaussian 03*, Revision C.02, Gaussian, Inc., Wallingford CT, USA, **2004**.
[29] a) M. J. Frisch, J. A. Pople, J. S. Binkley, *J. Chem. Phys.* **1984**, *80*, 3265–3269; b) A. D. McLean, G. S. Chandler, *J. Chem. Phys.* **1980**, *72*, 5639–5648; c) R. Krishnan, J. S. Binkley, R. Seeger, J. A. Pople, *J. Chem. Phys.* **1980**, *72*, 650–654.
[30] a) J. P. Foster, F. Weinhold, *J. Am. Chem. Soc.* **1980**, *102*, 7211–7218; b) A. E. Reed, L. A. Curtiss, F. Weinhold, *Chem. Rev.* **1988**, *88*, 899–926; c) A. E. Reed, F. Weinhold, *J. Chem. Phys.* **1983**, *78*, 4066–4073; d) A. E. Reed, F. Weinhold, *J. Chem. Phys.* **1985**, *83*, 1736–1740; e) A. E. Reed, R. B. Weinstock, F. Weinhold, *J. Chem. Phys.* **1985**, *83*, 735–746; f) F. Weinhold, J. E. Carpenter in *The Structure of Small Molecules and Ions*, Plenum, New York, **1988**.

Received: May 25, 2008
Published Online: October 13, 2008

